# Power effect on the properties of copper nitride films as solar absorber deposited in pure nitrogen atmosphere

M.I Rodríguez-Tapiador[1,*], J. Merino[2], T. Jawhari[3], A.L. Muñoz-Rosas[4], J. Bertomeu[4], S. Fernández[1,*]

[1]Energy Department, CIEMAT, Av. Complutense 40, Madrid 28040, Spain.
[2]University Rey Juan Carlos, Technology Support Center CAT, Tulipán, s/n, Móstoles 28039, Madrid, Spain
[3]Centres Científics i Tecnològics (CCiTUB), Universitat de Barcelona, Spain
[4]Departament de Física Aplicada, Universitat de Barcelona, Barcelona, Spain
[*]Correspondence:MariaIsabel.Rodriguez@ciemat.es;susanamaria.fernandez@ciemat.es

**Abstract**

Nowadays, the copper nitride ($Cu_3N$) is of great interest as a new solar absorber material, flexible and lightweight thin film solar cells. This material is a metastable semiconductor, non-toxic, composed of earth-abundant elements, and its band gap energy can be easily tunable in the range 1.4 to 1.8 eV. For this reason, it has been proposed for many applications in the solar energy conversion field. The main aim of this work is to evaluate the properties of the $Cu_3N$ thin films fabricated by reactive radio-frequency (RF) magnetron sputtering at different RF power values to determine its potential as light absorber. The $Cu_3N$ films were fabricated at room temperature (RT) from a Cu metallic target at the RF power ranged from 25 to 200 W onto different substrates (silicon and glass). The pure nitrogen flux was set to 20 sccm, and the working pressures were set to 3.5 Pa and 5 Pa. The XRD results showed a transition from (100) to (111) preferred orientations when RF power increased; the AFM images revealed a granular morphology, while FTIR and Raman spectra exhibited the characteristics peaks related to Cu-N bonds, which became narrower when the RF power increased. Finally, to stablish the suitability of these films as absorber, the band gap energy was calculated from transmission spectra.

**Graphical Abstract**

- Stable thin films of $Cu_3N$ were prepared at RT by reactive magnetron sputtering.A transition from (100) to (111) preferred orientation was observed as RF power increased.
- FTIR and Raman revealed the formation of Cu-N chemical bond, improved as RF power increased.
- The band gap energy values obtained were in the suitable range to use the material as solar absorber.

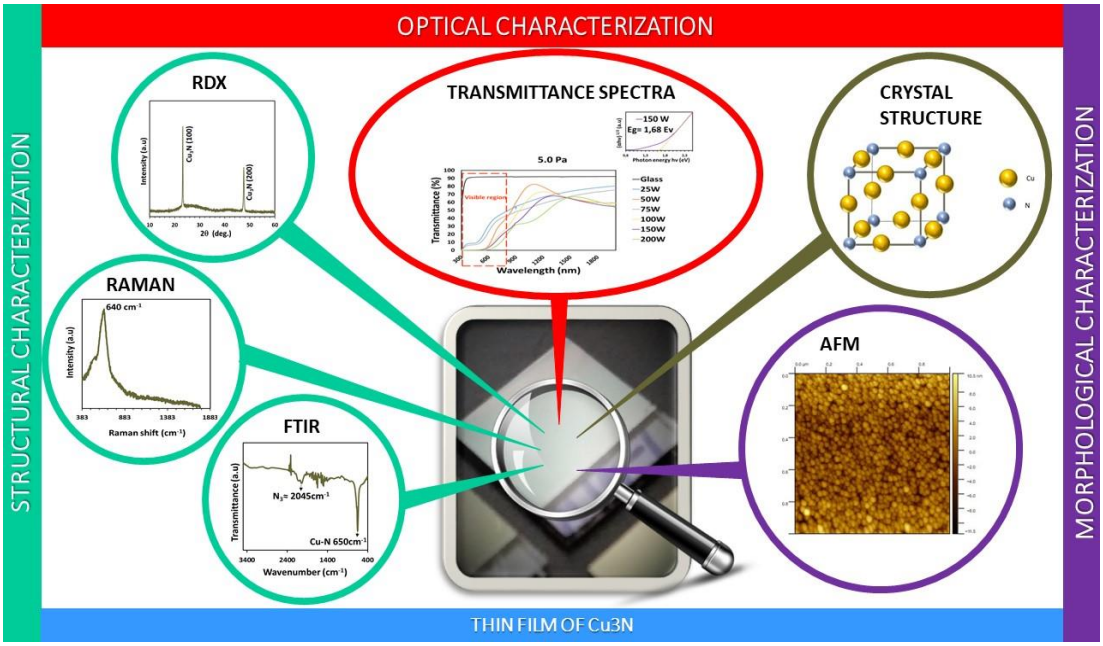


**Keywords:** Copper nitride, reactive magnetron sputtering, pure nitrogen atmosphere, absorber, photovoltaic devices.

Highlights:

- Stable thin films of $Cu_3N$ were prepared at RT by reactive magnetron sputtering. A transition from (100) to (111) preferred orientation was observed as RF power increased.
- FTIR and Raman revealed the formation of Cu-N chemical bond, improved as RF power increased.
- The band gap energy values obtained were in the suitable range to use the material as solar absorber.

## 1. Introduction

The $Cu_3N$ is of great interest as a new solar absorber material, flexible and lightweight thin film solar cells [1, 2]. This increasing interest as absorber for photovoltaic (PV) applications is due to the fact that is a metastable, non-toxic semiconductor, composed of earth-abundant elements, and its band gap energy can be easily tunable in the range 1.4 to 1.8 eV [3]. These solar-matches optical absorption ranges mean that the $Cu_3N$ film can be considered as a potential next-generation Earth abundant thin film solar cell absorber material and hence, as a possible substitute for the conventional silicon in a near future. Furthermore, this material can show both n and p-type character, which can be obtained by doping it with different elements that placed in interstitial position, such as fluorine [3]. Therefore, we can say that $Cu_3N$ fulfils the most of the required requirements for the next

generation of PV materials: earth-abundance, ecofriend, scalability, bipolar doping, suitable band gap energy and strong absorption, and beneficial transport properties.

$Cu_3N$ is a metastable semiconductor with an anti-$ReO_3$ cubic crystal structure [3]. The structure exhibits nitrogen (N) atoms at the corners of the cube and copper (Cu) atoms in the middle of each edge. The material is thermally and structurally stable at temperatures up to 200°C [4]. However, its thermal decomposition occurs in the temperature range of 100–470 °C [5]. In this sense, it has been reported that at high temperatures, visible structural changes can be appreciated and they may be related to the release of pure Cu [6].

The Cu-N family of bonding compounds can offer different optoelectronic properties, i.e. $Cu_4N$ that shows metallic behaviour, while $Cu_3N$ presents a semiconductor one, where there is a strong relationship between its chemical bonds and its electronic properties. These different behaviours can be achieved depending on the fabrication technique employed and modifying the deposition conditions. Such different behaviours are basically attributed to the vacant interstitial sites, because Cu atoms do not occupy the face-centred cubic (FCC) close packing sites[7]. Thanks to this, it is possible to tune the optoelectronic properties by incorporating different atoms in such vacant sites. In addition, the films can show different properties depending on the technique used. In this sense, chemical synthesis routes such as wet chemistry synthesis, solvothermal reactions of copper(II) chloride and sodium azide [8], the formation of $Cu_3N$ films by using urea and a nitrogen source [9] and other methods like ultrasonic and microwave [10], have been studied for several decades. In addition, physico-chemical fabrication methods have been also used for the $Cu_3N$ thin film deposition, e.g. molecular beam epitaxy (MBE) [11], pulsed magnetron sputtering (PMS) [12], pulsed laser deposition (RPLD) [13], and reactive direct current (DC) magnetron sputtering [14] or reactive radio-frequency (RF) magnetron sputtering [15-18]. Among them, the technique that offers higher scalability to the PV industry and improved homogeneity in large areas is magnetron sputtering, being therefore preferred to the chemical synthesis routes. In addition, in this last case, the film stoichiometry and the properties can be easily changed by modifying the main deposition parameters such as (i) the gas pressure, due to the interaction between N and Cu, which could modify the band gap [19], (ii) the substrate temperature and the power that can affect the structural, electrical and optical properties of the films [20], (iii) the type of the substrate [16], and (iv) the substrate to target distance, which can considerably vary the deposition rate [11]. Among these parameters, the plasma gas composition, commonly used a mixture of argon (Ar) and N, and the gas pressure both control the N fraction, and hence, the chemical composition of the deposited $Cu_3N$ thin film. Both parameters have a strong impact on the film structure, i.e. the lattice constant measured that can be ranged from 0.3815 to 0.3885 nm, and consequently, on their main optoelectronic properties such as band gap energy, absorbance and conductivity, especially relevant for photovoltaic applications [21].

In view of the above, in this work we evaluate the effect of the RF power on the structural and optoelectronic properties of $Cu_3N$ thin films sputtered at room temperature (RT) in a pure $N_2$ atmosphere, without introducing argon. In our previous work,we determined that the fact of not using Ar during the sputtering process led to the obtaining of $Cu_3N$ films with improved structural quality, with the (100) plane as preferential orientation and smoother surfaces than when using Ar-$N_2$ gas mixture as process gas [22]. For this reason, in this work, the N atmosphere is preferred.. It is expected to determine the optimized RF values and the N gas pressure range to obtain $Cu_3N$ films with appropriated morphologies, structures and band gap energies, suitable for the chosen application of emerging light absorber to replace silicon.. We show how these properties can be easily adjusted according to the requirements of the future device. Finally, it can be noticed that the

development of such earth-abundant thin-film material could have a significant cost advantage that could benefit its quick expansion in the PV industry thanks to the reduction of the amount of the material used and its availability and sustainability.

## 2. Materials and Methods

The deposition of the $Cu_3N$ thin films were carried out with a commercial MVSystem INC. monochamber sputtering system, where there is only one gun that can be vertically adjustable and is RF operated. The target used is a pure commercial Cu target (99.99%) with a 3-inch diameter, from Lesker Company. In this work, we used two types of substrates: 1737 Corning glass (Corning Inc., New York, USA) and <100> polished n-type floating zone crystalline silicon (c-Si) wafers. Prior to be loaded into the sputtering chamber, both substrates were prepared in a different way. The native silicon dioxide on the surface silicon wafer is removed with a 1% HF solution in deionized water and ethanol for 5 minutes. In the case of the glass, it was cleaned for 10 minutes in ultrasound, with ethanol and deionized water, and finally immersed in isopropyl alcohol. Subsequently, the substrates were dried by blowing nitrogen over them. After loading the substrates, the chamber was pumped to a pressure of $10^{-5}$ Pa. The working pressure was set to 3.5 and 5.0 Pa, adjusting it with a "butterfly" valve. The process gas was pure $N_2$ (purity 99.999%) at a flow rate of 20 sccm, controlled by a mass flow controller (MFC). The distance between the target and the substrate was set to 10 cm. $Cu_3N$ thin film depositions were performed at different powers ranged from 25 to 200W, and the deposition time was modified from 420 to 1800 s, depending the RF power value, to counteract the effect of the power on deposition rate.

The structure of the thin film was determined by X-ray diffraction (XRD), using a commercial Panalytical powder diffractometer model X'Pert MPD/MRD, with a Cu anode and secondary monochromator. The radiation used was Cu-kα radiation (λ=0.15406nm), and the scanned 2θ range was 10°-60° at a step size of 0.01°. To determine the chemical composition and molecular structure, Raman and Fourier transform infrared spectroscopy (FTIR) were used. Raman measurements were carried out with the dispersive spectrometer Horiba Jobin-Yvon LabRam HR 800 coupled, to an optical microscope Olympus BXFM, using a solid-state laser as an excitation source emitting at 532 nm. The Raman spectra were obtained with a laser power at the sample of about 5 mW and using a 100× microscope objectives. FT-IR measurements were carried out with a Perkin Elmer Spectrum 100 FT-IR in range of 400-4000 $cm^{-1}$. The morphology of the films was studied by atomic force microscopy (AFM) using an AFM model III A multimode nanoscope (Bruker). The roughness of the samples was determined from the root mean square (RMS) calculated with the commercial Gwyddion software. Finally, the optical properties were calculated from the transmittance spectra in the range 300-2000 nm, measured at RT and normal incidence with a Perkin Elmer Lambda 1050 spectrophotometer.

## 3. Results and discussion

Figure 1 shows the XRD spectra of the $Cu_3N$ films deposited on glass at different RF powers and at the different working pressures of 3.5 and 5.0 Pa. Regardless the pressure used, the XRD patterns show $Cu_3N$ crystallites with an anti-$ReO_3$ structure [23]. The $Cu_3N$ films deposited at low RF power values (below 150 W) present as preferential orientation the (100) plane that corresponds to the N-rich planes. As the RF power increases above 100 W, the intensity of the main (100) diffraction peak begins to decrease, while the (111) diffraction peak, corresponding to a Cu-rich plane [24], starts to appear as preferred from the sample deposited at 150 W [5]. In addition, this sample also presents several diffraction peaks of weaker intensity such as the (110) and (210) planes, referenced from the XRD

card number 00-047-1088 (The Joint Committee on Powder Diffraction Standards, 47–1088). This change observed in the phase transition orientation from the preferred (100) plane (around 23,3°) to the (111) (around 41°) one as the RF power increases can be attributed to the presence of a larger number of Cu atoms in the plasma. The high presence of Cu atoms could cause the formation of a $Cu_3N$ material saturated with Cu, which retains a cubic structure that begins to disappear and/or change at very high RF powers.

On the other hand, the main effect that the total pressure exerts on the films is the amorphous character, observed in the sample deposited at the highest pressure and the highest RF power of 200 W. Upon increasing the deposition pressure from 3.5 Pa to 5.0 Pa produces more N ions, are bombarding the Cu target, leading to a higher amount of Cu ions or atoms in the plasma, with the $Cu^{2+}$ and $Cu^{+}$ ionization states. The sample deposited at 200 W and 5.0 Pa shows amorphous structure, in comparison with that deposited at 200 W and 3.5 Pa. This can be attributed to a high presence of Cu atoms, because of the high RF power, that would reach the substrate surface with less energy due to the increase of the collisions between the particles within the plasma at the increased pressure The saturation effect of the Cu in the film at higher pressures is more evident. This is the reason why the Cu-rich phase disappears. In addition, under these extreme conditions, there is an increase in ion bombardment, resulting in more defects produced in the sputtered films. This indicates that the film crystallinity is seriously deteriorated, due to the excessive RF power and subsequently, excessive amount of Cu atoms, giving rise to amorphous $Cu_3N$ material. Conversely, at low RF power values, more $N^{+2}$ and $N^{+}$ free radicals are generated due to the high proportion of low-energy electrons that are formed in the plasma[18]. Hence, the samples deposited at low RF powers show the preferential N-rich planes, and a better crystal quality [25].

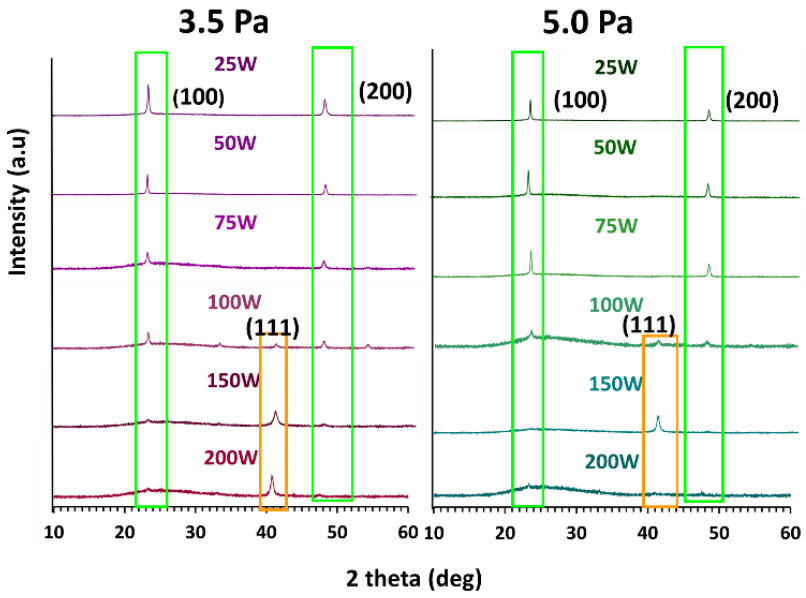


Figure 1. X-ray diffraction pattern of $Cu_3N$ films deposited at different RF Power and the working pressure of 3.5 Pa (left) and 5.0 Pa (right).

Molecular information about the chemical structure of $Cu_3N$ thin films were obtained by Raman and FTIR techniques. These two techniques are very useful to give information on the vibrational state of the molecular bonds found in the films, and they are considered as complementary. It is well-know that the position of this peak is dependent on the stoichiometry of $Cu_xN$ layers, that in the case of Raman, ranging from 635 to 610 $cm^{-1}$ for

the N/Cu ratio as it decreases. [26] As shown the Figure 2 and Figure 3, the FTIR and Raman peaks reveal the formation of $Cu_3N$ because of the position in which the main peaks are observed [27, 28]. The Figure 2 shows the FTIR spectra of the films as function of the RF power values, where a band around the wavenumber of 650 $cm^{-1}$ was observed, being the typical peak of the stretching vibrations attributed to Cu-N bonds[29]. The peaks at 5.0 Pa are wider than the ones obtained at 3.5 Pa, and closer to 650 $cm^{-1}$, while the band of the samples deposited at 150 and 200 W is quite far from the ≈ 650 $cm^{-1}$, revealing the change in their structure. On the other hand, the Figure 3 depicts the Raman spectra where the typical bands of $Cu_3N$ thin films, found at the wavelength of ≈ 634$cm^{-1}$ [30], are the characteristic ones of Cu-N bonds [31]. A slight shift to lower wavenumbers is observed when the RF power increases, attributed to deviation from the stoichiometric level more evident at high RF powers where the $Cu_3N$ structure is Cu-rich [32]. Whereas, the sample deposited at 200 W and 5.0 Pa presents a Raman spectrum completely different, which can be attributed to the appearance of $CO_2$ and/or CO absorption bands [33].

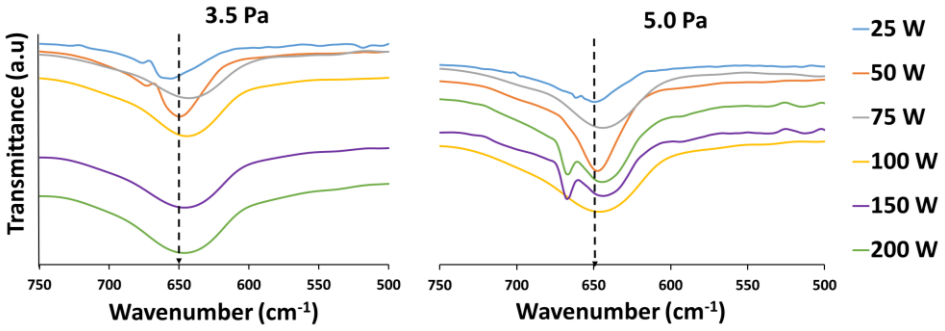


Figure 2. FTIR spectra of $Cu_3N$ films prepared by magnetron sputtering at different RF power and the working pressures of 3.5 Pa and 5.0 Pa.

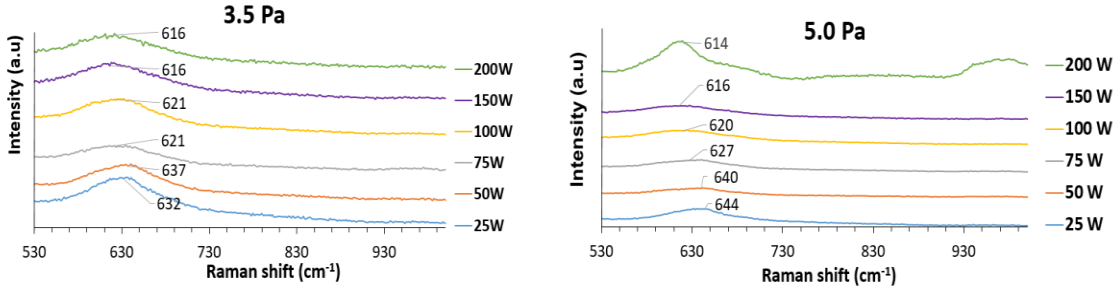


Figure 3. The Raman spectra of $Cu_3N$ films prepared by magnetron sputtering at different RF power and the working pressures of 3.5 Pa and 5.0 Pa.

The surface of the samples was analysed by AFM. The scanning area was 1x1$\mu m^2$. Figure 4 shows the surface roughness obtained from the root-mean-square (rms) as function of the RF power. As it can be observed, the higher the rms value, the rougher the surface of the thin film. It was also observed that the smoothest films with close-grained surface morphology were the surface of the samples made at 5.0 Pa and lower RF power values.

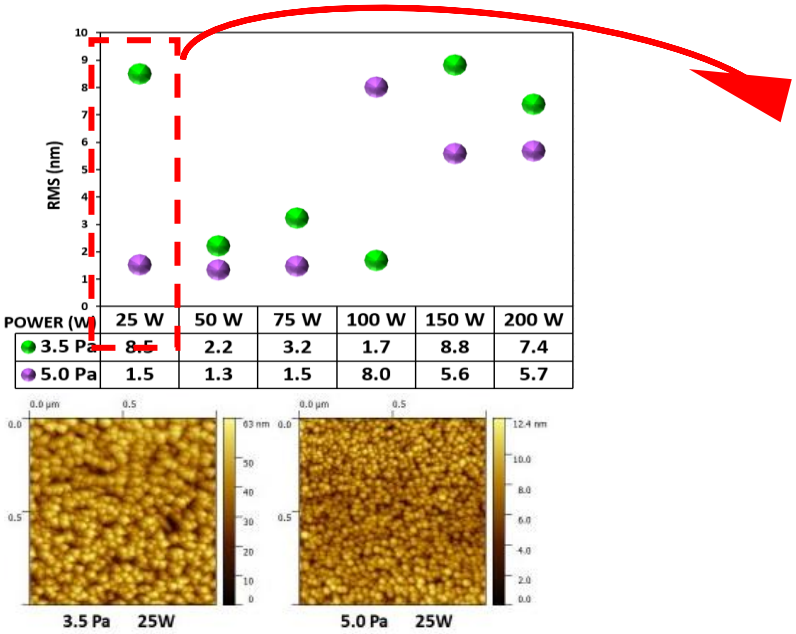


Figure 4. Rms values (nm) calculated vs RF power at different working pressures of 3.5 Pa and 5.0 Pa.

Finally, the optical properties of $Cu_3N$ thin films deposited on glass substrates were analysed by UV-VIS-NIR spectroscopy in the range of 300-2000nm. Figure 5 pictures the transmittance spectra of the deposited thin films at 3.5 Pa and 5.0 Pa, where a greater number of fringes appear as RF power increases, attributed to the thicker films obtained by increasing the deposition rate with the RF power. These spectra clearly show a low transparency of the films in the visible region, and a maximum optical transmission close to 80%, showed for the samples deposited at low values of RF power, in the near infrared region.

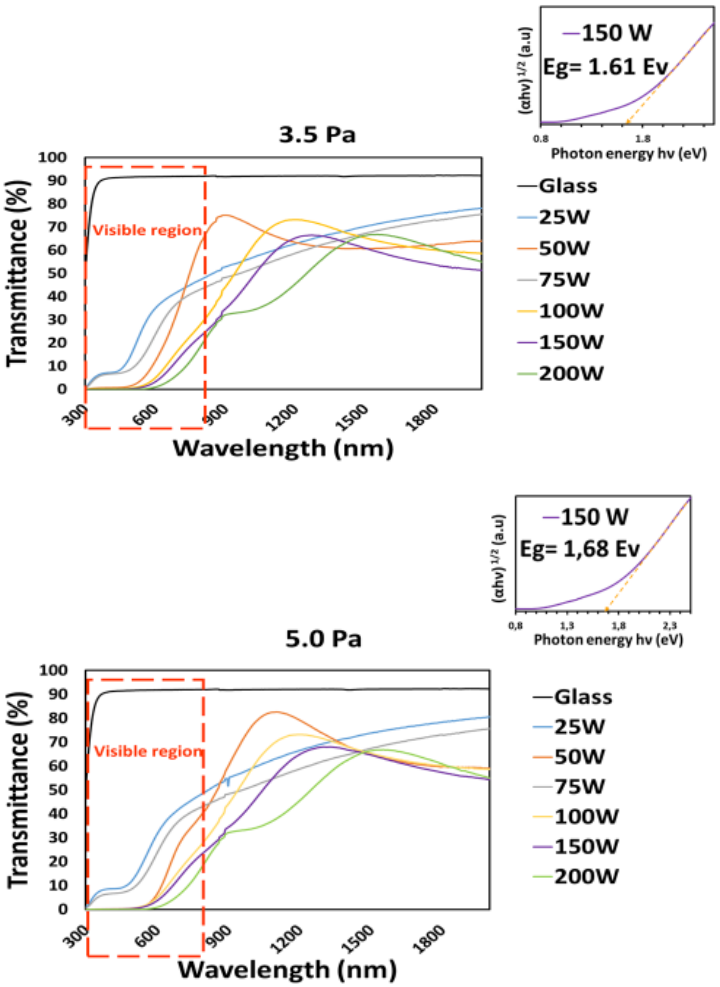


Figure 5. Transmittance spectra of the $Cu_3N$ in study. In the inset, representative $(h\nu\alpha)^{1/2}$ vs hν plots of the sample deposited at 150 W, for the determination of the direct and indirect band gap.

From the transmittance spectra and the Tauc equation [34], the band gap of the $Cu_3N$ films were calculated, with the aim of determining their potential as solar absorbers.

$(h\nu\alpha)^{1/}$ $A(h$ $Eg)$ Eq. 1

where A is the band tailing parameter and p is the parameter associated with type of transition, i.e. p=2 for an indirect allowed transition and p=1/2 is direct allowed transition, α is the absorption coefficient, and hν is photon energy. In the inset of Figure 5, the $(h\nu\alpha)^{1/2}$ vs hν plots for the samples deposited to 3.5 Pa and 5.0 Pa, at 150 W are pictured as example. Table 1 summarised the values of the direct and indirect band energies obtained varying the RF power. They are very close to those found in the literature [12, 34]. In the case of the samples deposited at 3.5 Pa, we observe a slightly blue-shift in the band gap energy as the RF power increases. This may be attributed to the increasing presence of unbonded Cu atoms, which would form a defect level, leading to a reduction in the band gap. We would be faced with the effect of Cu supersaturation. However, in the case of the samples deposited at 5.0 Pa, that tendency is not so well appreciated. This leads us to believe that the Cu oversaturation effect would not be occurring due to the increase of the gas pressure [35].

Table 1. Direct and indirect band gap calculated by using Tauc plot for the samples deposited at different RF powers and a total pressure of 3.5 Pa and 5.0 Pa, respectively.

| | | | **3.5 Pa** | | | |
|---|---|---|---|---|---|---|
| **RF Power (W)** | 25 | 50 | 75 | 100 | 150 | 200 |
| **Band Gap Eg (eV)** | | | | | | |
| **Direct $(\alpha h\nu)^2$** | 2.16 | 2.12 | 2.04 | 2.08 | 2.04 | 2.04 |
| **Indirect $(\alpha h\nu)^{1/2}$** | 1.90 | 1.80 | 1.70 | 1.76 | 1.61 | 1.68 |

| | | | **5.0 Pa** | | | |
|---|---|---|---|---|---|---|
| **RF Power (W)** | 25 | 50 | 75 | 100 | 150 | 200 |
| **Band Gap Eg (eV)** | | | | | | |
| **Direct $(\alpha h\nu)^2$** | 2.12 | 2.12 | 2.04 | 2.04 | 2.04 | 2.04 |
| **Indirect $(\alpha h\nu)^{1/2}$** | 1.68 | 1.80 | 1.68 | 1.68 | 1.68 | 1.72 |

## 4. Conclusions

This work presents the optimization of the sputtering deposition of $Cu_3N$ thin films using a $N_2$ pure environment, at RT and at different RF power values with the aim to determine its suitability as optical absorber. XRD patterns reveal a change in the preferred orientation from (100) to (111) as increasing the RF power. Moreover, at RF power of 100 W and above, a polycrystalline structure with the presence of several weak diffraction peaks are obtained. From the chemical point of view, FTIR and Raman measurements confirmed the presence of Cu-N bonds. From AFM images, it is observed that thin films prepared at low RF power and 3.5 Pa show very smooth surfaces. Finally, the direct and indirect band gap values calculated are suitable for solar absorbers. Hence, these results indicate that (i) the magnetron sputtering is an appropriate method to fabricate this kind of material, and (ii) the depositions at low RF power (up to 100 W) and $N_2$ pressures of 3.5 Pa are mainly preferred due to its smoother surfaces, its stoichiometry closer to the required one, and suitable band gap energies that permit to use this material as a potential absorber substitute of silicon.

## 5. Acknowledgements

This research has been supported by Grants PID2019-109215RB-C42 and PID2019-109215RB-C43 funded by MCIN/AEI/ 10.13039/501100011033.

M.A. Rodríguez-Tapiador also acknowledge partial funding through MEDIDA C17.I2G: CIEMAT. Nuevas tecnologías renovables híbridas, Ministerio de Ciencia e Innovación, Componente 17 “Reforma Institucional y Fortalecimiento de las Capacidades del Sistema Nacional de Ciencia e Innovación”. Medidas del plan de inversiones y reformas para la recuperación económica funded by the European Union – NextGenerationEU. The authors would also like to thank A. Soubrie from Centro de Microscopía Electrónica “Luis Bru” for her advice and AFM measurements. Finally, A.L. Muñoz-Rosas is grateful to SECTEI México for granted postdoctoral fellowship.

**Conflict of Interest:**

No, there is no conflict of interest.

**Data Availability Statement:**

Research data are not shared.

## 6. References


1. Noh, H.; An, H.; Lee, J.; Song, J.; Hong, H. J.; Seo, S.; Jeong, S. Y.; Kim, B.-J.; Ryu, S.; Lee, S., Large enhancement of the photocurrent density in N-doped Cu3N films through bandgap reduction. *Journal of the Korean Ceramic Society* **2020,** 57, (3), 345-351. DOI:
2. Tilemachou, A.; Zervos, M.; Othonos, A.; Pavloudis, T.; Kioseoglou, J., p-Type Iodine-Doping of Cu3N and Its Conversion to γ-CuI for the Fabrication of γ-CuI/Cu3N pn Heterojunctions. *Electronic Materials* **2022,** 3, (1), 15-26. DOI:
3. Caskey, C. M.; Richards, R. M.; Ginley, D. S.; Zakutayev, A., Thin film synthesis and properties of copper nitride, a metastable semiconductor. *Mater. Horiz.* **2014,** 1, (4), 424-430. DOI: 10.1039/c4mh00049h.
4. Okrasa, S.; Wilczopolska, M.; Strzelecki, G.; Nowakowska-Langier, K.; Chodun, R.; Minikayev, R.; Król, K.; Skowronski, L.; Namyślak, K.; Wicher, B., The influence of thermal stability on the properties of Cu3N layers synthesized by pulsed magnetron sputtering method. *Thin Solid Films* **2021,** 735, 138889. DOI: https://doi.org/gmrdwf.
5. Borsa, D. M.; Boerma, D. O., Growth, structural and optical properties of Cu3N films. *Surface Science* **2004,** 548, (1-3), 95-105. DOI: https://doi.org/bvbwb4.
6. Zakutayev, A., Design of nitride semiconductors for solar energy conversion. *Journal of Materials Chemistry A* **2016,** 4, (18), 6742-6754. DOI: https://doi.org/gh77ds.
7. Sahoo, G., Site selective Ag doping in Cu3N and its consequences on structural and electronic properties: A DFT study. *Physica B: Condensed Matter* **2021,** 619, 413238. DOI:
8. Choi, J.; Gillan, E. G., Solvothermal synthesis of nanocrystalline copper nitride from an energetically unstable copper azide precursor. *Inorganic chemistry* **2005,** 44, (21), 7385-7393. DOI:
9. Ohigashi, Y.; Higuchi, A.; Rosero-Navarro, N. C.; Miura, A.; Tadanaga, K., Preparation of Cu 3 N thin films by nitridation of solution process-derived thin films using urea. *Journal of Sol-Gel Science and Technology* **2022**, 1-5. DOI:
10. Goktas, S.; Goktas, A., A comparative study on recent progress in efficient ZnO based nanocomposite and heterojunction photocatalysts: A review. *Journal of Alloys and Compounds* **2021,** 863, 158734. DOI:
11. Asano, M.; Umeda, K.; Tasaki, A., Cu3N thin film for a new light recording media. *Japanese Journal of Applied Physics* **1990,** 29, (10R), 1985. DOI: doi: https://doi.org/cb9mcn
12. Wilczopolska, M.; Nowakowska-Langier, K.; Okrasa, S.; Skowronski, L.; Minikayev, R.; Strzelecki, G. W.; Chodun, R.; Zdunek, K., Synthesis of copper nitride layers by the pulsed magnetron sputtering method carried out under various operating conditions. *Materials* **2021,** 14, (10), 2694. DOI: https://doi.org/gmkmxh.
13. Gallardo-Vega, C.; De la Cruz, W., Study of the structure and electrical properties of the copper nitride thin films deposited by pulsed laser deposition. *Applied surface science* **2006,** 252, (22), 8001-8004. DOI: https://doi.org/cptf9f.
14. Majumdar, A.; Drache, S.; Wulff, H.; Mukhopadhyay, A. K.; Bhattacharyya, S.; Helm, C. A.; Hippler, R., Strain effects by surface oxidation of Cu3N thin films deposited by DC magnetron sputtering. *Coatings* **2017,** 7, (5), 64. DOI:
15. Zamani Meymian, M. R.; Delavari Heravi, A.; Kosari Mehr, A., Influence of bias voltage on optical and structural characteristics of Cu3N films deposited by reactive RF magnetron sputtering in a pure nitrogen atmosphere. *Materials*

*Science in Semiconductor Processing* **2020,** 112, 104995. DOI: 10.1016/j.mssp.2020.104995.
16. Razeghizadeh, A.; Mahmoudi Ghalvandi, M.; Sohillian, F.; Rafee, V., The Effect of Substrate on Structural and Electrical Properties of Cu3N Thin Film by DC Reactive Magnetron Sputtering. *Physical Chemistry Research* **2017,** 5, (3), 497-504. DOI:
17. Chen, S.-C.; Huang, S.-Y.; Sakalley, S.; Paliwal, A.; Chen, Y.-H.; Liao, M.-H.; Sun, H.; Biring, S., Optoelectronic properties of Cu3N thin films deposited by reactive magnetron sputtering and its diode rectification characteristics. *Journal of Alloys and Compounds* **2019,** 789, 428-434. DOI: 10.1016/j.jallcom.2019.02.268.
18. Park, H.; Seo, H.; Kim, S. E., Anti-oxidant copper layer by remote mode N2 plasma for low temperature copper–copper bonding. *Scientific reports* **2020,** 10, (1), 1-13. DOI: https://doi.org/jpb5
19. <Design of nitride semiconductors for solar energy conversion.pdf>. DOI: 10.1039/x0xx00000x.
20. Fioretti, A. N.; Schwartz, C. P.; Vinson, J.; Nordlund, D.; Prendergast, D.; Tamboli, A. C.; Caskey, C. M.; Tuomisto, F.; Linez, F.; Christensen, S. T.; Toberer, E. S.; Lany, S.; Zakutayev, A., Understanding and Control of Bipolar Self-Doping in Copper Nitride. *J Appl Phys* **2016,** 119, (18). DOI: 10.1063/1.4948244.
21. Xiao, J.; Qi, M.; Cheng, Y.; Jiang, A.; Zeng, Y.; Ma, J., Influences of nitrogen partial pressure on the optical properties of copper nitride films. *RSC Advances* **2016,** 6, (47), 40895-40899. DOI: 10.1039/c6ra03479a.
22. Figueira, C.; Rosario, G. D.; Pugliese, D.; Rodríguez-Tapiador, M.; Fernández, S., Effect of Argon on the Properties of Copper Nitride Fabricated by Magnetron Sputtering for the Next Generation of Solar Absorbers. *Materials* **2022,** 15, (24), 8973. DOI: doi.org/10.3390/ma15248973.
23. Zhou, X.; Gall, D.; Khare, S. V., Mechanical properties and electronic structure of anti-ReO3 structured cubic nitrides, M3N, of d block transition metals M: An ab initio study. *Journal of alloys and compounds* **2014,** 595, 80-86. DOI:
24. Wang, J.; Chen, J.; Yuan, X.; Wu, Z.; Miao, B.; Yan, P., Copper nitride (Cu3N) thin films deposited by RF magnetron sputtering. *Journal of Crystal Growth* **2006,** 286, (2), 407-412. DOI: https://doi.org/10.1016/j.jmst.2018.02.025.
25. Rodríguez-Tapiador, M.; Merino, J.; Jawhari, T.; Muñoz-Rosas, A.; Bertomeu, J.; Fernández, S., Impact of the RF Power on the Copper Nitride Films Deposited in a Pure Nitrogen Environment for Applications as Eco-Friendly Solar Absorber. *Materials* **2023,** 16, (4), 1508. DOI:
26. Park, J.-M.; Jin, K.; Han, B.; Kim, M. J.; Jung, J.; Kim, J. J.; Lee, W.-J., Atomic layer deposition of copper nitride film and its application to copper seed layer for electrodeposition. *Thin Solid Films* **2014,** 556, 434-439. DOI:
27. Maksimov, O.; Gong, X.; Gordon, R. G.; Hijazi, H.; Bhandari, H., Atomic Layer Deposition of Cu3n Using Copper Dimethylamino-2propoxide and Ammonia. *Available at SSRN 4234247*. DOI:
28. Singh, K., Magnetic and spectroscopic studies on cupric azide. *Transactions of the Faraday Society* **1971,** 67, 2436-2444. DOI:
29. Du, Y.; Ji, A.; Ma, L.; Wang, Y.; Cao, Z., Electrical conductivity and photoreflectance of nanocrystalline copper nitride thin films deposited at low temperature. *Journal of crystal growth* **2005,** 280, (3-4), 490-494. DOI: doi:10.1016/j.jcrysgro.2005.03.077.
30. Fallberg, A.; Ottosson, M.; Carlsson, J.-O., Phase stability and oxygen doping in the Cu–N–O system. *Journal of crystal growth* **2010,** 312, (10), 5. DOI:
31. Sajeev, A.; Paul, A. M.; Nivetha, R.; Gothandapani, K.; Gopal, T. S.; Jacob, G.; Muthuramamoorty, M.; Pandiaraj, S.; Alodhayb, A.; Kim, S. Y.; Van Le, Q.; Show, P. L.; Jeong, S. K.; Grace, A. N., Development of Cu3N electrocatalyst for hydrogen

evolution reaction in alkaline medium. *Sci Rep* **2022,** 12, (1), 2004. DOI: 10.1038/s41598-022-05953-x.

32. Nowakowska-Langier, K.; Chodun, R.; Minikayev, R.; Okrasa, S.; Strzelecki, G. W.; Wicher, B.; Zdunek, K., Phase composition of copper nitride coatings examined by the use of X-ray diffraction and Raman spectroscopy. *Journal of Molecular Structure* **2018,** 1165, 79-83. DOI: https://doi.org/gmrdwq
33. Zervos, M.; Othonos, A.; Pavloudis, T.; Giaremis, S.; Kioseoglou, J.; Mavridou, K.; Katsikini, M.; Pinakidou, F.; Paloura, E. C., Impact of Oxygen on the Properties of Cu3N and Cu3–x N1–x O x. *The Journal of Physical Chemistry C* **2021,** 125, (7), 3680-3688. DOI: https://doi.org/gpnd7m.
34. Jiang, A.; Qi, M.; Xiao, J., Preparation, structure, properties, and application of copper nitride (Cu 3 N) thin films: A review. *Journal of Materials Science & Technology* **2018,** 34, (9), 1467-1473. DOI: 10.1016/j.jmst.2018.02.025.
35. Chen, Y.-H.; Lee, P.-I.; Sakalley, S.; Wen, C.-K.; Cheng, W.-C.; Sun, H.; Chen, S.-C., Enhanced Electrical Properties of Copper Nitride Films Deposited via High Power Impulse Magnetron Sputtering. *Nanomaterials* **2022,** 12, (16), 2814. DOI: